A comparison of ground-based and airborne SAR systems for the detection of landmines, UXO and IEDs

Andreas Heinzel*[a], Markus Schartel[b], Ralf Burr[c], Rik Bähnemann[d], Eric Schreiber[a], Markus Peichl[a], Christian Waldschmidt[b]

[a]German Aerospace Center (DLR), Muenchener Strasse 20, 82234 Wessling, Germany; [b]University of Ulm, Albert-Einstein-Allee 41, 89081 Ulm, Germany; [c]Ulm University of Applied Sciences, Albert-Einstein-Allee 55, 89081 Ulm, Germany; [d]ETH Zurich, Leonhardstrasse 21, 8092 Zürich, Switzerland.

ABSTRACT

The task of detecting and locating landmines, unexploded ordnances (UXO) and improvised explosive devices (IEDs) is still a major challenge up to the present day. Problems such as the distance between the hazardous area and the measurement system as well as the differentiation between the target of interest and the surrounding soil are of importance in the development of the sensor system. Various types of radar based systems have been developed over the last decades to solve these problems. Compared to other methods ground penetrating synthetic aperture radar (SAR) has the ability to scan large areas from a safe standoff distance in a relatively short time. In this paper, two different imaging radar systems are compared. The first one is a ground-based SAR (GB-SAR) developed at German Aerospace Center (DLR). The other system is an unmanned aerial vehicle-based SAR (UAV-SAR) from the University of Ulm. The presented data originates from a joint campaign using the same measurement scenarios.

Keywords: Landmine Detection, Ground Penetrating Synthetic Aperture Radar, Ground-Based Radar, Unmanned Aerial Vehicle Radar

1. INTRODUCTION

The problem of a high number of regions being contaminated with landmines, UXO and IEDs has led to the development of various sensing technologies over the last decades. Devices like metal detectors, ground penetrating radars as well as acoustic or chemical sensors have been investigated. Though these sensor systems are proven to generate reliable data, the close proximity to the explosive targets is often a major concern. In addition, the measurement principles result in a low area throughput. Compared to that, ground penetrating SAR has the ability to scan large areas from a safe, standoff distance in a relatively short time. Furthermore, a high resolution in three spatial dimensions can be achieved resulting in a precise localization of the objects. A multi-static or multi-look approach enables an enhanced clutter suppression that is necessary for the detection of these threats. Clutter from the soil has typically a more statistical behavior than man-made objects resulting in a gain in the signal-to-clutter ratio when different viewing angles are covered. The two systems discussed here are independent developments of DLR and the University of Ulm. The GB-SAR (DLR) can be set up on a rail wagon or truck and consists of a digital pulse radar with two transmit and four receive channels, [1] [2]. The UAV-SAR incorporates a single radar channel with separate transmit and receive antennas and allows for a flexible choice of flight patterns to enhance the chance of detecting targets, [3] [4]. Besides the different hardware setups, the image processing algorithm used in both systems relies on the backprojection algorithm which leads to comparable data products, [5]. The results of a joint measurement campaign conducted at the DLR site in Oberpfaffenhofen Germany are discussed within this work. The underlying, identical measurement scenarios allow for a fair and comprehensive analysis of the two different system concepts.

2. SYSTEM CONCEPTS

In this chapter the basic hardware parameters are presented. Figure 1 shows images of the two systems and a detailed overview of the system parameters is given in table 1.

The setup of the GB-SAR from DLR working under a side looking geometry is shown on the lower left side of Figure 1. The system is build up on a rail wagon and consists of two independent transmit and four receive channels resulting in eight different radar images. The antenna array consists of six logarithmic periodic antennas. The frequency range is 500 MHz to 3 GHz with a transmit power of 0 dBm. Linear frequency modulated up-chirps with a pulse duration of 1 μs and a repetition frequency of 40 Hz are used. The position data are obtained by a special algorithm using three markers observed a stationary optical camera.

The UAV-SAR of University of Ulm is shown on the right bottom of Figure 1. As carrier platform a DJI Matrice 600 Pro is used. The FMCW radar operates in a frequency range from 1 GHz to 4 GHz with a transmit power of 15 dBm. The signal duration time is 1.024 ms and the repetition frequency is approximately 30 Hz. A stationary laser tracker aimed at a prism mounted below the UAV and an inertial measurement unit (IMU) are used to retrieve the position and orientation of the UAV in space.

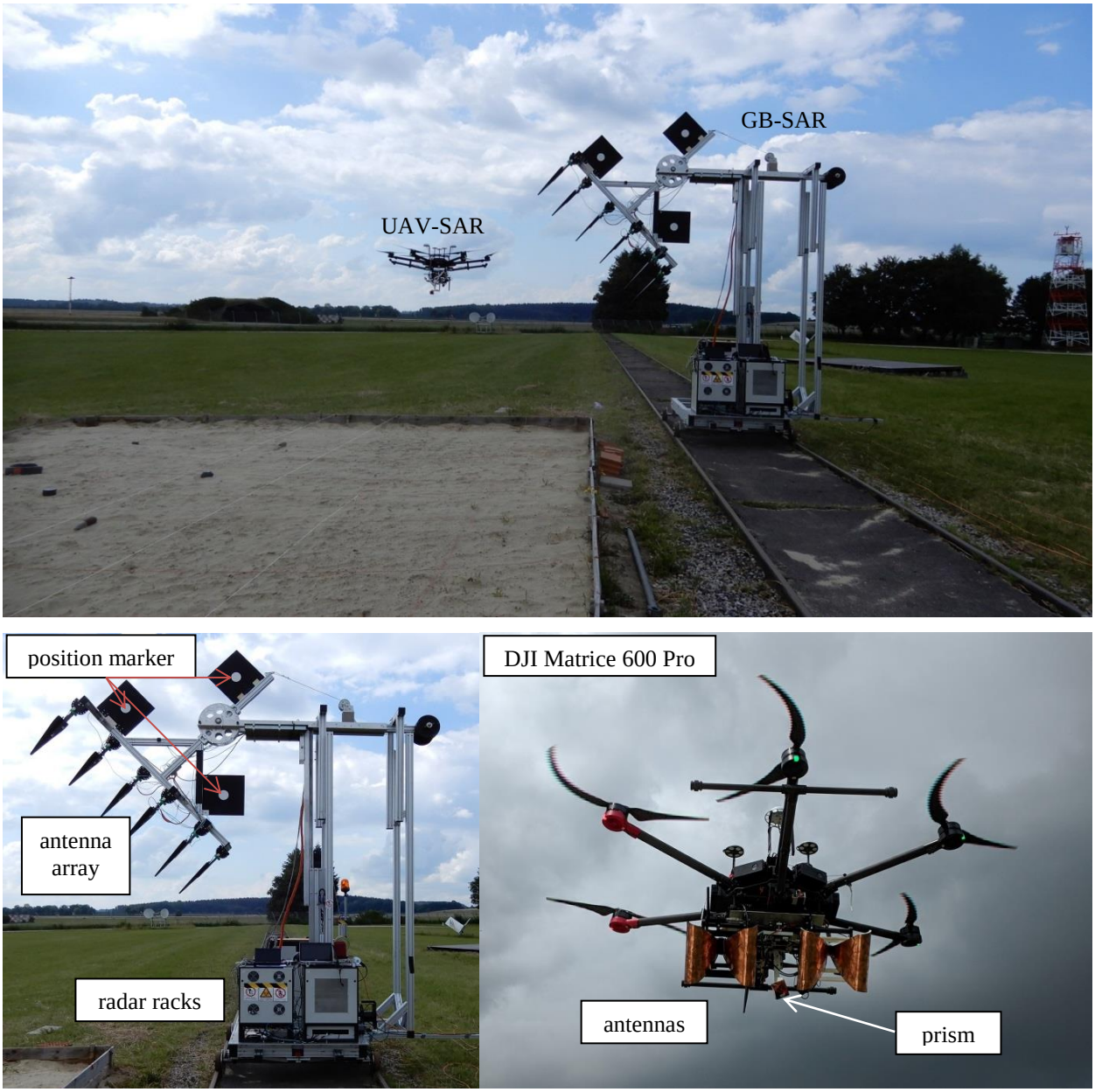

Figure 1. Hardware setup GB-SAR from DLR (left) and UAV-SAR from University of Ulm (right).

Table 1. Measurement parameter for GB-SAR and UAV-SAR.

Measurement parameter	GB-SAR	UAV-SAR
Frequency range	0.5-3 GHz	1-4 GHz
Signal time duration	1 µs	1.024 ms
Transmit power	0 dBm	15 dBm
Pulse repetition frequency	40 Hz	30 Hz
Sampling distance azimuth	0.0025 m	0.0535 m

3. MEASUREMENT RESULTS

In the following, results of measurements performed at the DLR facility in Oberpfaffenhofen using horizontal and vertical polarized antennas are shown and compared. Both systems observe the target area from the same side and operate using a linear trajectory. Different targets are placed within a sandbox surrounded by grassland.

3.1 Measurement Setup

In Figure 2 photographs of the measurement scenario and test objects are shown. A total of 12 different landmines, UXOs as well as a pressure plate are used for the measurement campaign. The objects are first placed on the surface (see Figure 2) and then buried near the surface in a depth of approximately 5 cm. Four trihedral reflectors are used as reference among all images but are cut out in the radar images.

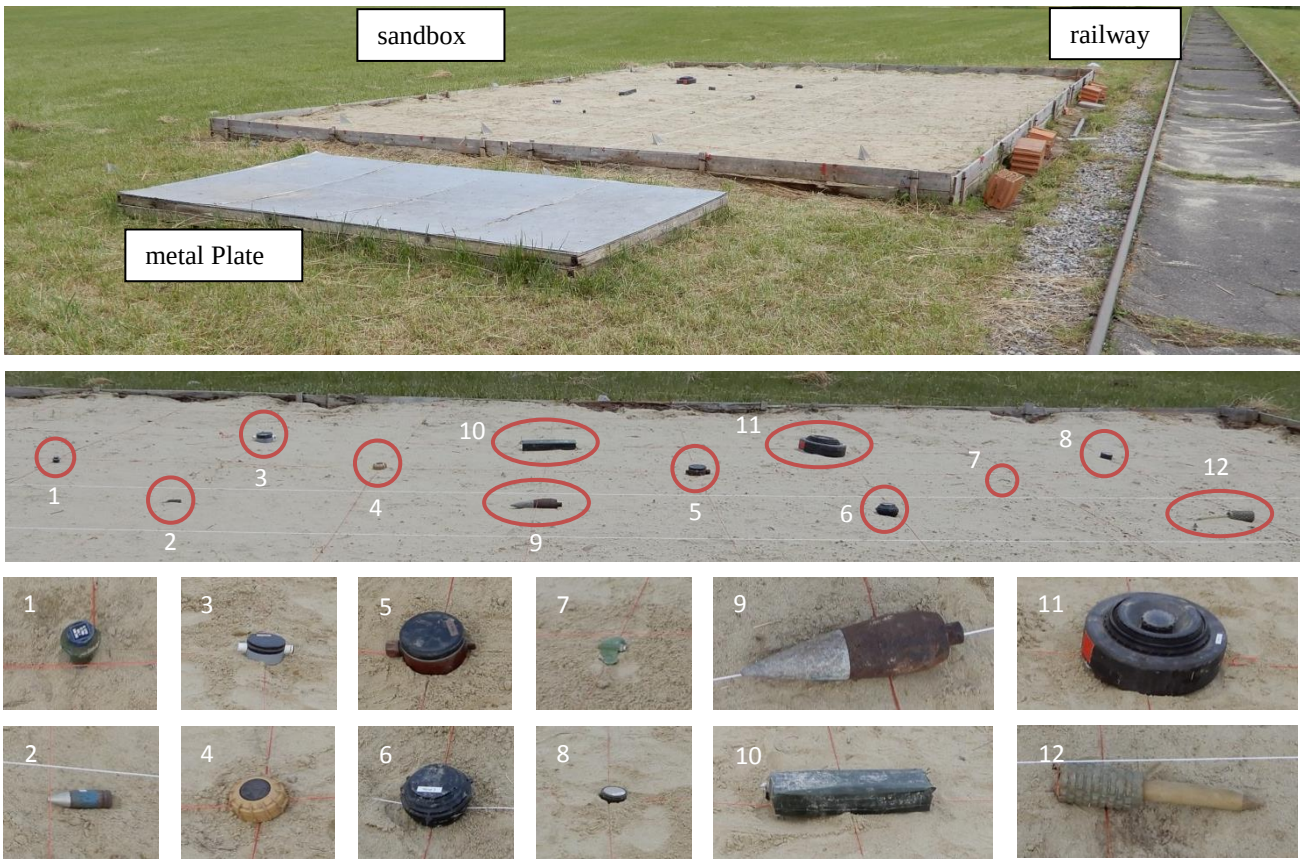

Figure 2. Measurement scenario with objects on the surface of the sandbox.

Table 2. Types of landmines used in measurement scenario and their material.

index	**1**	**2**	**3**	**4**	**5**	**6**
type of landmine	C3A2	munition	PMN	VS-50	PMN	PMA
material	Plastic	metal	bakelit	plastic	bakelit	plastic
index	**7**	**8**	**9**	**10**	**11**	**12**
type of landmine	PFM-1S	DM18B1	grenade	pressure plate	PT-Mi-Ba-III	PMR
material	metal	metal	metal	wood	bakelit	metal

3.2 Measurement Procedure and Results

In this chapter the measurement procedure and results for the scenario and objects illustrated in chapter 3.1 are shown. The measurements were carried out one after the other from the same viewing side. The UAV flights were performed manually, resulting in a deviation of the flight paths compared to the movement of the antennas of the GB-SAR. At the time of the measurement campaign the UAV-SAR was not able to produce fully coherent radar images. Therefore, only radar images as a result of an incoherent superposition (amplitude only) for trajectories in different heights are shown. In the histograms also results of a coherent superposition (amplitude and phase) of the GB-SAR are considered in order to see the quality improvement by having a full coherence. The coherent superposition results in a better resolution compared to the incoherent summation and leads to a better localization of the object in space. Therefore targets focus in different heights which make it difficult to illustrate in a clear manner. In the case of GB-SAR, eight independent images, one for each Tx-Rx antenna combination, are superimposed and in case of the UAV-SAR a summation over five flight paths has been done. The movement of the GB-SAR was much smoother compared to the UAV due to the strong wind and the manually performed flights. Therefore a better focusing is achieved by GB-SAR resulting in a better resolution and a clearer RCS structure.

In Figure 3 results of objects placed on the surface and in Figure 4 of objects buried in a depth of approximately 5 cm with horizontal polarization (a) and (b) and vertical polarization (c) and (d) are shown. The result (a) and (c) are from the UAV-SAR and (b) and (d) are results of the GB-SAR. The amplitudes are normalized to the maximum of the strongest scatterer in the images which is either object 9 or 12 and represented in a logarithmic scale. The targets 9 and 12 are metallic have the largest visible radar cross section (RCS). The dynamic range was deliberately set differently in the individual images in order to increase the visibility of the targets in case of the buried targets. The smallest RCS has landmine 1 which is completely out of plastic. The advantage of detecting objects on the surface is the double bounce of the electromagnetic wave between the object and the surface. This effect vanishes when objects are buried. Target 11, for example, is an anti-tank mine that has a strong double bounce in the horizontal polarization. When this object is buried (Figure 4) this effect disappears which results in a much lower RCS. Another aspect is the orientation of the objects to the radar. Target 4 is most visible in horizontal polarization whereas target 7 can only be seen in vertical polarization. This result shows that it is beneficial to use different polarizations in order to increase the chance of detecting objects due to their polarimetric scattering behavior. In Figure 5 and Figure 6 histograms of the amplitudes of the images in Figure 3 and Figure 4 are shown. The blue curve corresponds to the UAV-SAR (incoherent), the red curve to the GB-SAR (incoherent), and in green the curve of the GB-SAR (coherent) is shown. In case of the coherent superposition only targets at the selected depth are shown. The amplitudes are normalized to the strongest target in the scenery and the sum over the amplitude density is one. On the right side a bar shows the maximum amplitudes of each of the 12 targets in the scenery. The values are ordered from top to bottom from the weakest to the strongest. In case of targets with weak scattering behavior the highest value close to the assumed location of the respective object is chosen. The amplitudes of the targets in the UAV-SAR case are often higher but also the clutter has higher values. For detection the maximum amplitude of the target response is not decisive, the ration between signal-to-clutter is more important. The higher the difference the better the chance of detection with less false alarms. It can also be seen in the histograms that the clutter for vertical polarization is higher than for horizontal polarization. Another important aspect is the fact that some targets differ strongly in the amplitudes between UAV-SAR and GB-SAR. For example target 11 appears much stronger on the surface for the UAV-SAR and target 12 is stronger visible for GB-SAR in the buried case with horizontal polarization. The coherent superposition results in a different shape of the distribution for the clutter having a much lower mean value. Although targets sometimes have lower amplitudes compared to the incoherent case the difference between target amplitude and clutter is still higher resulting in a better detection. Therefore a full coherent radar is desirable.

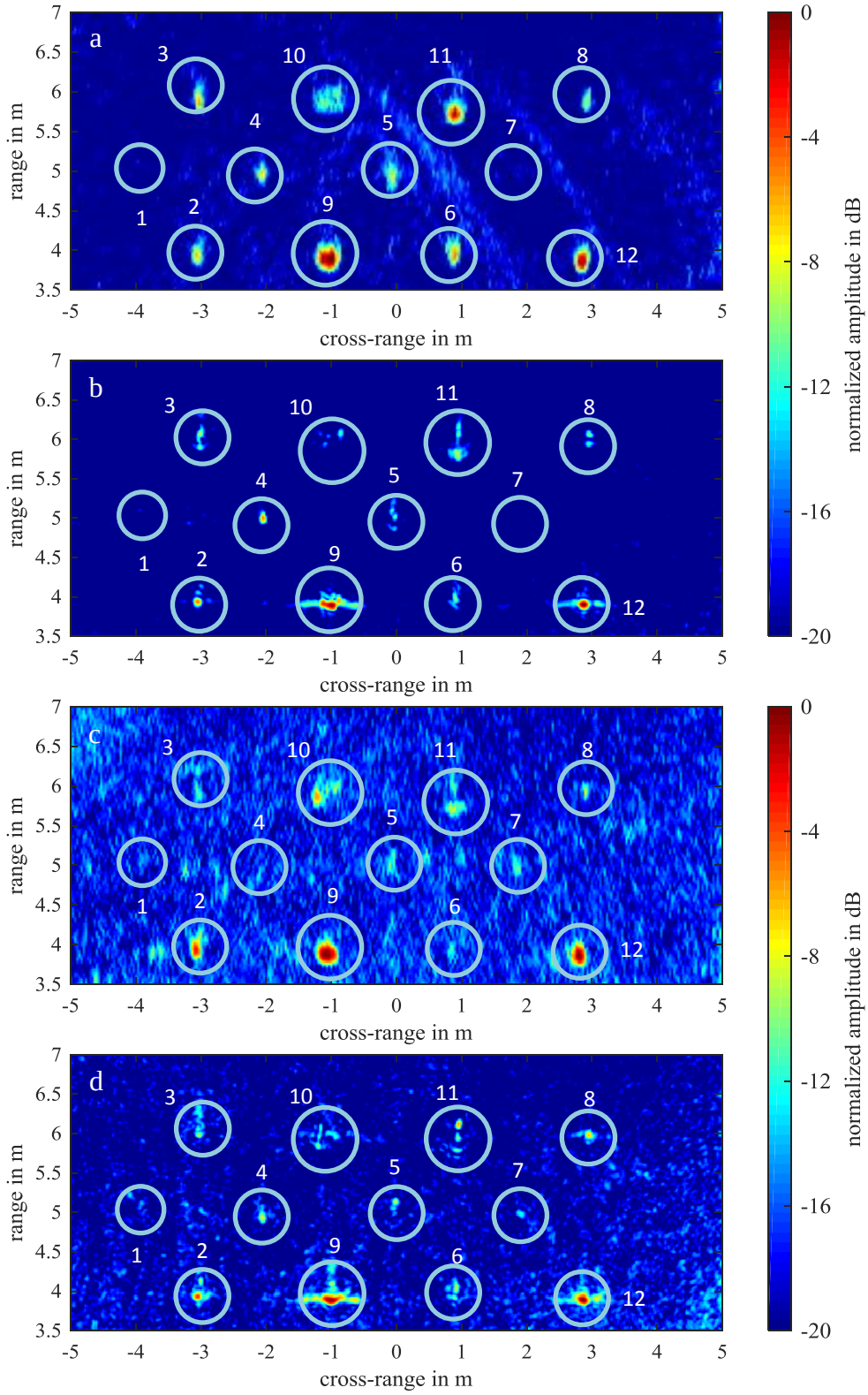

Figure 3. Measurement result of objects on the surface with horizontal polarization (a) and (b) and vertical polarization (c) and (d). The result (a) and (c) are from the UAV-SAR and (b) and (d) are results of the GB-SAR.

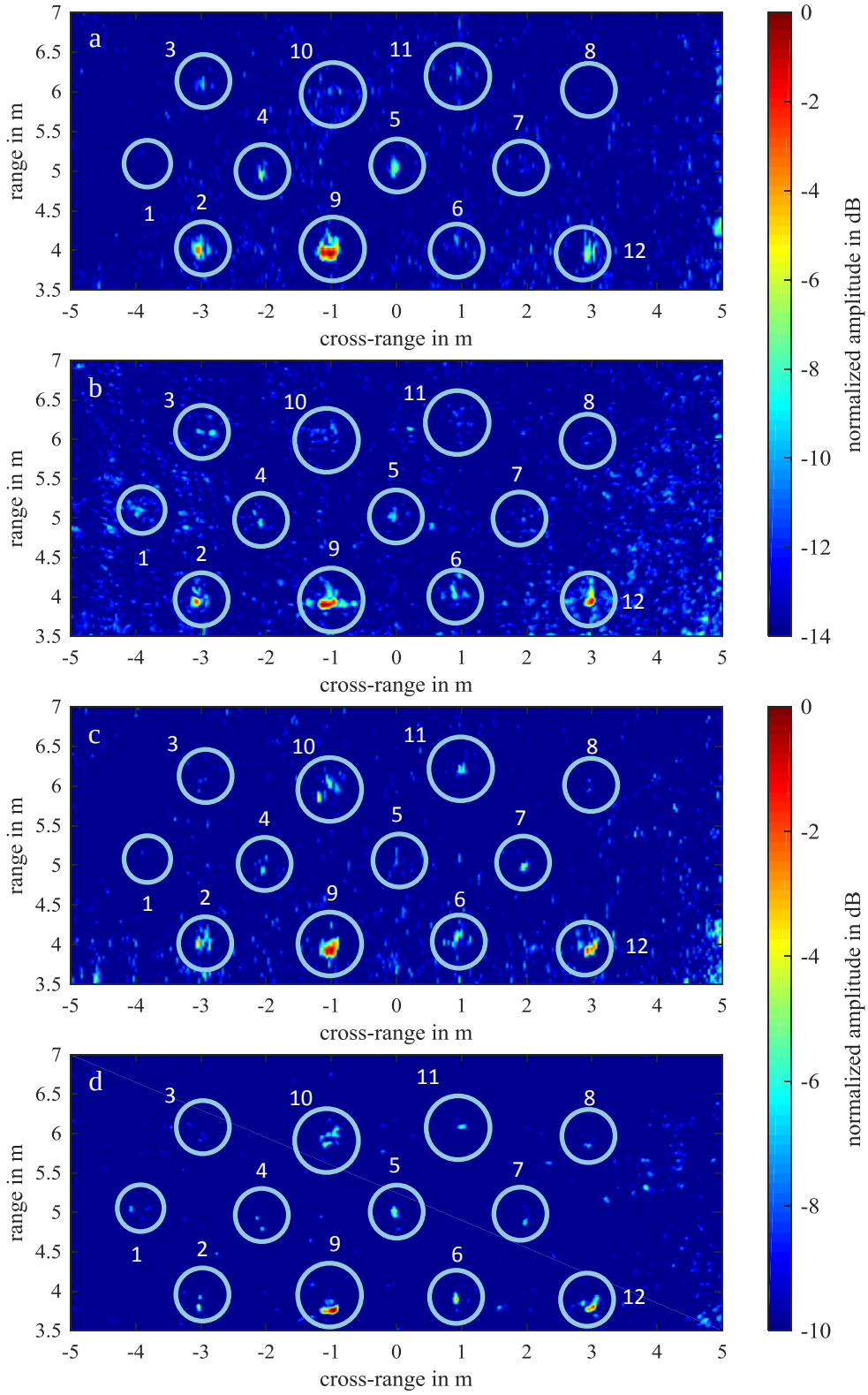

Figure 4. Measurement result of buried objects with horizontal polarization (a) and (b) and vertical polarization (c) and (d). The result (a) and (c) are from the UAV-SAR and (b) and (d) are results of the GB-SAR.

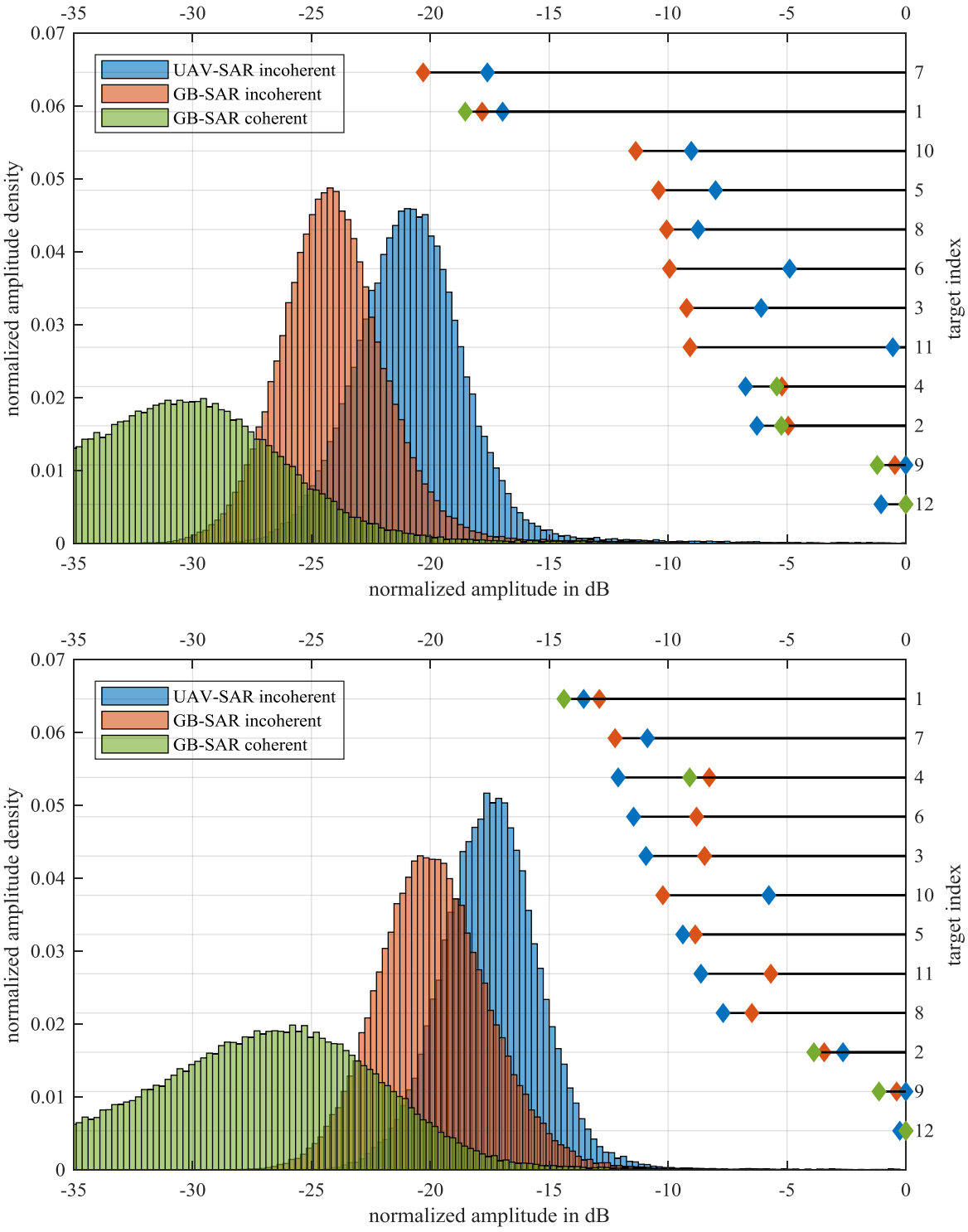

Figure 5. Histogram of UAV-SAR incoherent (blue), GB-SAR incoherent (red) and GB-SAR coherent (green) of the normalized amplitudes of the images from the surface. The values are normalized to the strongest target in the image and the sum over the amplitude density is one. The bar on the right indicates the amplitudes of the different targets in the scenery with the index shown in the right y-axis. Horizontal polarization (top) and vertical polarization (bottom).

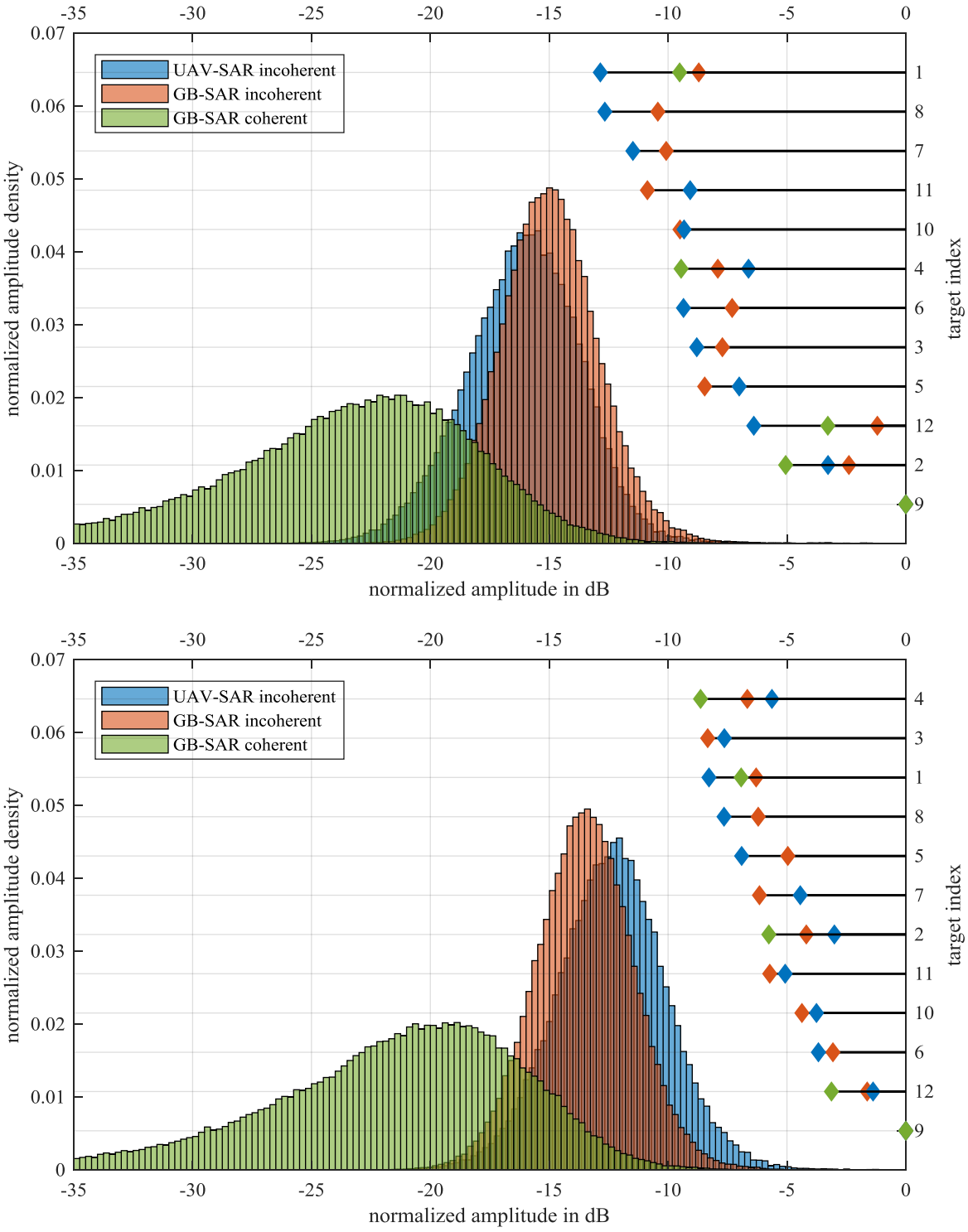

Figure 6. Histogram of UAV-SAR incoherent (blue), GB-SAR incoherent (red) and GB-SAR coherent (green) of the normalized amplitudes of the images from the buried objects. The values are normalized to the strongest target in the image and the sum over the amplitude density is one. The bar on the right indicates the amplitudes of the different targets in the scenery with the index shown in the right y-axis. Horizontal polarization (top) and vertical polarization (bottom).

4. CONCLUSION AND OUTLOOK

Results of a joint measurement campaign have shown that SAR with different elevation angles has the ability to detect threats over large areas with high resolution in a relatively short time. Different viewing angles as well as polarimetry are necessary to have a high detection rate while reducing false alarms. GB-SAR and UAV-SAR have shown reliable results due to the high accuracy of the radar and motion compensation. The better calibration and position estimation in case of GB-SAR result in a higher performance. Nevertheless the performance could further be improved by UAV-SAR using more advanced trajectories like circular ones to suppress the clutter even better and also get a better reconstruction of the shape of an object. The challenge for future UAV-SAR is therefore to get a full coherence combined with a precise position estimation of the radar.

REFERENCES

[1] Schreiber, E., Peichl, M., Heinzel, A., Dill, S., and Bischeltsrieder, F., "Detection of landmines and UXO using advanced synthetic aperture radar technology," Proc. SPIE 9823, Detection and Sensing of Mines, Explosive Objects, and Obscured Targets XXI, 98231S, 2016.

[2] Schreiber, E., Peichl, M., Heinzel, A., Dill, S., "Challenges for operational use of ground-based high-resolution SAR for landmines and UXO detection," EUSAR Conference, 2016.

[3] Burr, R., Schartel, M., Schmidt, P., Mayer, W., Walter, T. and Waldschmidt, C., "Design and Implementation of a FMCW GPR for UAV-based Mine Detection," International Conference on Microwaves for Intelligent Mobility (ICMIM), 2018.

[4] Schartel, M., Burr, R., Mayer, W., Docci, N., and Waldschmidt, C., "UAV-Based Ground Penetrating Synthetic Aperture Radar," International Conference on Microwaves for Intelligent Mobility (ICMIM), 2018.

[5] Halevy, S., "Tomographic Radar Imaging Techniques," Twenty-Second Asilomar Conference on Signals, Systems and Computers, Pacific Grove, 1988.